Effect of nonhydrostatic stresses on solid-fluid equilibrium. II. Interface thermodynamics

T. Frolov* and Y. Mishin†
Department of Physics and Astronomy, MSN 3F3, George Mason University, Fairfax, Virginia 22030, USA
(Received 13 August 2010; published 16 November 2010)

We investigate thermodynamics of single-component solid-fluid interfaces when the solid phase is subject to nonhydrostatic mechanical stresses. The analysis reveals that when the solid is nonhydrostatic, the interface stress is not unique. We show the existence of several types of interface stresses, formulate them as interface excess quantities, and establish relationships between them. Using molecular dynamics simulations with an empirical potential, we compute several different interface stresses for a (110) solid-liquid interface in copper. The simulations show that biaxial tension and compression of the solid produce a strong effect on the magnitude, sign, and anisotropy of the interface stresses. The free energy of the interface was computed by thermodynamic integration along biaxial tension and compression paths. The effect of nonhydrostatic stresses on the interface free energy is much weaker than the effect on interface stresses.

DOI: 10.1103/PhysRevB.82.174114 PACS number(s): 68.35.Md, 68.08.De, 67.80.bf, 62.50.−p

I. INTRODUCTION

Solid-fluid interfaces occur in wide variety of physical phenomena and technological processes.[1] In many situations, the solid phase is subject to nonhydrostatic mechanical stresses. At present, there is no clear understanding of how such stresses can affect interface properties. The goal of this work is to perform a rigorous analysis of interface thermodynamics in the presence of nonhydrostatic stresses in the solid. As in Part I of this work dedicated to bulk thermodynamics of nonhydrostatic systems,[2] we study a simple case of a single-component material as an example. We also perform atomistic simulations in order to verify some of our theoretical results and to evaluate the relative strength of different effects predicted by the analysis.

Thermodynamics of interfaces was founded by Gibbs.[3] To define thermodynamic quantities characterizing an interface, Gibbs developed the concept of a dividing surface. He introduced the quantity γ, referred to nowadays as interface free energy, as reversible work required to create a unit area of interface. He expressed this quantity through excesses, relative to a chosen diving surface, of other extensive thermodynamic properties such as energy, entropy, and the numbers of atoms of different chemical components. Using this formalism of excesses, Gibbs derived the celebrated adsorption equation expressing the differential of γ through differentials of intensive properties characterizing the phase coexistence. Analyzing solid-fluid interfaces, Gibbs pointed out that the interface area can be varied by elastic stretching of the solid phase. The work of such stretching is done by what is now called the interface stress $\hat{\tau}$.

Gibbs showed that a nonhydrostatically stressed single-component solid can be equilibrated with three multicomponent fluids each having a different chemical potential of the solid component.[3] This implies that the chemical potential of the solid component cannot be defined uniquely. Gibbs circumvented the problem of the undefined chemical potential by placing the dividing surface so that the interface excess of the solid component would vanish. This eliminates the term in the adsorption equation that would otherwise require knowledge of a chemical potential. As was pointed out by Cammarata,[4,5] this would be impossible for a solid solution with a variable chemical composition.

Using the Gibbsian definition of γ, Cahn[6] derived a more general form of the adsorption equation for hydrostatic systems by solving a system of Gibbs-Duhem equations for the bulk phases and a layer containing the interface. Cahn's method affords a greater freedom of choice of the intensive variables used in the adsorption equation. It rigorously introduces the interface excess volume, a quantity which is zero by definition in the Gibbsian treatment. The freedom of choice of variables and the conjugate interface excess quantities offers significant advantages for experimental and computational applications. Another advantage of Cahn's method[6] is that the Gibbs phase rule is directly embedded in the formalism, making all variations in the adsorption equation automatically consistent with phase coexistence.

Recently, Cahn's treatment[6] was extended to nonhydrostatic solids and applied to study single-component solid surfaces and binary solid-fluid interfaces.[7,8] The adsorption equation was rederived in a form which includes elastic variations in the interface area and thus introduces the interface stress tensor. The latter appears in the adsorption equation as an excess of the stress tensor over bulk stresses existing inside the phases. An interface version of the Gibbs-Helmholtz equation was also derived, offering a variety of thermodynamic integration paths along the phase coexistence surface in the configuration space of variables.

A relation between γ and $\hat{\tau}$ was first established for a single-component solid surface by Shuttleworth.[9] In this simple case, arbitrary lateral strains can be applied at a constant temperature, performing work against $\hat{\tau}$ and changing γ. By contrast, elastic deformations of a solid-fluid interface cannot be arbitrary but must satisfy the phase coexistence conditions. For example, in a single-component system, elastic stretching at a constant temperature and pressure in the fluid can result in complete melting/evaporation of the solid phase. Such prohibited strains cannot be used in a definition of the interface stress and cannot appear in the Shuttleworth equation.

In this paper we analyze possible elastic deformations of a solid-fluid interface which are consistent with phase equilib-

rium. The interface stress tensor is defined through an appropriate term in the adsorption equation. This term represents the work of reversible elastic deformation of the interface without violating the phase coexistence. For a given initial state of a two-phase system, there are multiple paths on the phase coexistence surface, each corresponding to a different physical process, on which the interface area can change elastically. The work of stretching along different paths is generally different, making $\hat{\tau}$ a nonunique thermodynamic quantity. We analyze different definitions of the interface stress implied by the adsorption equation and compute three of such stresses using atomistic computer simulations.

Most of the thermodynamic quantities appearing in the adsorption equation cannot be directly measured in experiments but are readily accessible by computer simulations. The interface free energy along phase coexistence paths was previously computed for several single-component and binary solid-liquid interfaces using the cleaving technique,[10,11] the capillary fluctuation method,[12–14] various thermodynamic integration schemes,[7,8,15,16] and other approaches.[17,18] For curved interfaces, γ was computed from modeling of homogeneous nucleation events.[19–21] However, previous atomistic studies of solid-liquid interfaces were restricted to systems in which the solid was either unstressed or stressed hydrostatically (or nearly hydrostatically). In this work we apply atomistic simulations to compute γ and different interface stresses $\hat{\tau}$ along strongly nonhydrostatic coexistence paths. Such paths were obtained by equilibration of a biaxially strained solid with its melt at a constant zero pressure p in the melt. When designing and interpreting our simulations, we used results for nonhydrostatic solid-fluid equilibrium between bulk phases presented in Part I of this work.[2]

The rest of the paper is organized as follows: in Sec. II we analyze interface thermodynamics of nonhydrostatic single-component systems. After introducing our atomistic simulation methodology in Sec. III, we present the simulation results in Sec. IV and draw conclusions in Sec. V.

II. THERMODYNAMICS OF SOLID-FLUID INTERFACES

A. Interface free energy γ and the adsorption equation

1. Interface free energy

Consider a rectangular block containing a single-component solid under a general state of mechanical stress in thermodynamic equilibrium with a fluid of the same component (Fig. 1). The solid-fluid interface is planar and perpendicular to the z direction of the block. Thermal equilibrium between the phases requires that temperature T be uniform throughout the system. Due to mechanical equilibrium, the principal component σ_{33}^s of the stress tensor σ_{ij}^s in the solid is perpendicular to the interface and equal to negative pressure p in the fluid. The phase-change equilibrium condition relates properties of the solid to the chemical potential μ^f in the fluid,[3]

$$U^s - TS^s + pV^s = \mu^f N^s, \tag{1}$$

where U^s, S^s, V^s, and N^s are the energy, entropy, volume, and number of atoms of an arbitrary homogeneous region of the solid phase. For any homogeneous region of the fluid phase we have

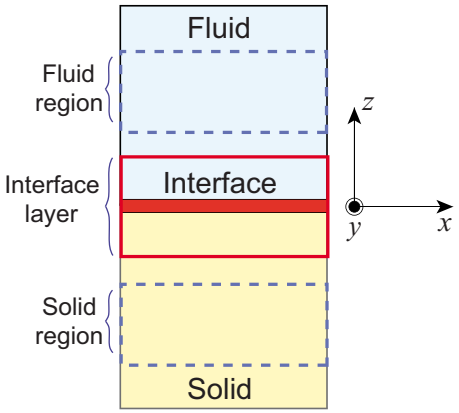

FIG. 1. (Color online) Schematic of a solid-fluid system with a plane interface. The interface layer and the homogeneous solid and fluid regions are outlined.

$$U^f - TS^f + pV^f = \mu^f N^f, \tag{2}$$

where U^f, S^f, V^f, and N^f are the energy, entropy, volume, and number of atoms of the fluid region. Examples of homogeneous regions inside the phases are illustrated in Fig. 1.

Consider a layer containing the solid-fluid interface (Fig. 1). The choice of this layer is arbitrary as long as its boundaries are placed inside of homogeneous parts of the solid and fluid phases. Using Gibbs' definition of the interface free energy[22] in conjunction with Eqs. (1) and (2), it can be shown that[3]

$$\gamma A = U - TS + pV - \mu^f N, \tag{3}$$

where U, S, V, and N are the total energy, entropy, volume, and number of atoms in the layer and A is the physical area of the interface. The extensive quantities U, S, V, and N are not physically meaningful interface properties because they depend on the choice of the boundaries of the layer. To eliminate this dependence, we solve the system of three Eqs. (1)–(3) for γA using Cramer's rule of linear algebra. This results in the following expression for γA in terms of interface excesses of extensive properties:[8]

$$\gamma A = [U]_{XY} - T[S]_{XY} + p[V]_{XY} - \mu^f [N]_{XY}. \tag{4}$$

Here X and Y are any two out of four extensive properties U, S, V, and N. In Eq. (4) and other equations appearing below, $[Z]_{XY}$ denotes the ratio of two determinants[6]

$$[Z]_{XY} \equiv \frac{\begin{vmatrix} Z & X & Y \\ Z^s & X^s & Y^s \\ Z^f & X^f & Y^f \end{vmatrix}}{\begin{vmatrix} X^s & Y^s \\ X^f & Y^f \end{vmatrix}}. \tag{5}$$

The quantities appearing in the first row of the 3×3 determinant are computed for the chosen layer containing the interface whereas the quantities with superscripts s and f are computed for homogeneous regions in the solid and fluid

phases, respectively. It can be shown that $[Z]_{XY}$ is equal to the excess of property Z when the interface is formed by joining two solid and fluid regions and the system obtained contains the same amounts of properties X and Y as the initial phases combined. Importantly, $[Z]_{XY}$ does not depend on the choice of the boundaries of the layer or the bulk regions,[6] making it a physically meaningful interfacial quantity. A the same time, $[Z]_{XY}$ does generally depend on the choice of the extensive properties X and Y. When two columns in the 3×3 determinant in Eq. (5) are identical, the excess is zero

$$[X]_{XY} = [Y]_{XY} = 0. \tag{6}$$

In other words, excesses of the properties X and Y are identically zero. Due to Eq. (6), two terms in the right-hand side of Eq. (4) are eliminated by specifying X and Y, leaving only two nonzero terms.

For example, if $X=N$ and $Y=V$, the total interface free energy becomes $\gamma A=[U]_{NV}-T[S]_{NV}$. If we choose $X=N$ and $Y=S$, then $\gamma A=[U]_{NS}+p[V]_{NS}$. Thus, by choosing different extensive properties X and Y we can express γA as an excess of different thermodynamic potentials

$$\gamma A = [U - TS]_{NV} = [U + pV]_{NS} = \cdots \tag{7}$$

Equation (7) shows that while the excesses of U, S, V, and N depend on the choice of X and Y, γA is unique.

2. Adsorption equation

Our next goal is to derive a differential equation for reversible variations in γA in terms of variations in intensive properties. Consider a closed solid-fluid block, as in Fig. 1, containing a fixed number of unit cells of the solid in the cross section parallel to the interface (in other words, a fixed Lagrangian area of the interface). Consider a reversible variation in state of the system in which it can receive/release heat and do mechanical work by changing its shape and dimensions, including changes in the physical area of the interface by elastic deformation. Differentiating Eqs. (1)–(3) one can derive the following Gibbs-Duhem-type equations for the interface layer and the bulk solid and fluid regions

$$d(\gamma A) = -SdT + Vdp - Nd\mu^f + \sum_{i,j=1,2} (\sigma_{ij} + \delta_{ij}p)Vd\epsilon_{ij}, \tag{8}$$

$$0 = -S^s dT + V^s dp - N^s d\mu^f + \sum_{i,j=1,2} (\sigma^s_{ij} + \delta_{ij}p)V^s d\epsilon_{ij}, \tag{9}$$

$$0 = -S^f dT + V^f dp - N^f d\mu^f. \tag{10}$$

Here, σ_{ij} is the stress tensor averaged over the layer and ϵ_{ij} is a symmetrical 2×2 lateral strain tensor computed relative to the current state. We are assuming that the distorted shape of the block is triclinic, hence $d\epsilon_{ij}$ is the same in all three equations. For a detailed derivation of Eqs. (8) and (9) we refer the reader to Refs. 7 and 8. [Gibbs derived Eq. (9) for a more general case of finite deformations.][3]

The differentials appearing in the right-hand side of Eq. (8) are not independent. They are subject to constraints imposed by thermodynamic equilibrium between the bulk phases and expressed by Eqs. (9) and (10).[6] Solving the system of these three equations, we obtain the adsorption equation expressing a variation in the total interface free energy γA in terms of independent intensive variables[7]

$$d(\gamma A) = -[S]_{XY}dT + [V]_{XY}dp - [N]_{XY}d\mu^f + \sum_{i,j=1,2} [(\sigma_{ij} + \delta_{ij}p)V]_{XY}d\epsilon_{ij}. \tag{11}$$

The excess quantities $[Z]_{XY}$ appearing in Eq. (11) are computed by Eq. (5), where Z, X, and Y are three out of the extensive properties S, V, N, and $(\sigma_{ij}+\delta_{ij}p)V$. By specifying X and Y, two terms in Eq. (11) are eliminated, leaving four variables that can be varied independently.[23]

It is important to note that some choices of the extensive properties X and Y are prohibited by Cramer's rule. For example, if $X=(\sigma_{11}+p)V$ and $Y=(\sigma_{22}+p)V$, then $X^f=Y^f=0$ and the excess $[Z]_{XY}$ of any property Z is undefined. This restriction on the choice of X and Y originates from the fact that the solid and fluid phases have different numbers of degrees of freedom: two for the fluid and five for the solid.[24] The Gibbs-Duhem equation for the fluid phase, Eq. (10), does not contain the lateral strain variables. As a result, only one strain variable can be eliminated from the system of three equations but not two. Thus, the four degrees of freedom of the solid-fluid system can be represented by four intensive variables from the set $(T,p,\mu^f,\epsilon_{11},\epsilon_{22},\epsilon_{12})$, with the requirement that at least two of them are strain components.

B. Interface stress

1. Definition and multiplicity of interface stresses

In this section we analyze different interface stresses introduced through the adsorption equation. By choosing different extensive variables X and Y in Eq. (11), several forms of the adsorption equation can be obtained, each having a different set of independent variables and leading to different definitions of the interface stress. Indeed, the change in γA due to elastic work done by or against interface stress is represented by the last term in Eq. (11). From this term we can express $\hat{\tau}$ as an excess of the tensor $(\sigma_{ij}+\delta_{ij}p)V$ over its bulk values on either side of the interface

$$\tau^{XY}_{ij} = \frac{1}{A}\frac{\partial(\gamma A)}{\partial \epsilon_{ij}} = \frac{1}{A}[(\sigma_{ij} + \delta_{ij}p)V]_{XY} = \frac{1}{A}\frac{\begin{vmatrix} (\sigma_{ij} + \delta_{ij}p)V & X & Y \\ (\sigma^s_{ij} + \delta_{ij}p)V^s & X^s & Y^s \\ 0 & X^f & Y^f \end{vmatrix}}{\begin{vmatrix} X^s & Y^s \\ X^f & Y^f \end{vmatrix}}, \tag{12}$$

where $i,j=1,2$.[25] The variables held constant during the variation in ϵ_{ij} depend on the choice of X and Y. The only case when the interface stress is independent of X and Y is when the solid is hydrostatic, in which case $\sigma^s_{ij}+\delta_{ij}p=0$ and τ_{ij} has a unique value $\tau_{ij}=(\sigma_{ij}+\delta_{ij}p)V/A$.

To further demonstrate that the interface stress is not unique if the solid is nonhydrostatic, we will consider ex-

amples of different choices of X and Y. Three examples will be given in this section and one more in Sec. II B 2.

First, let $X=V$ and $Y=N$. The adsorption equation becomes

$$d(\gamma A) = -[S]_{NV}dT + \sum_{i,j=1,2}[(\sigma_{ij}+\delta_{ij}p)V]_{NV}d\epsilon_{ij} \quad (13)$$

with four independent variables T, ϵ_{11}, ϵ_{12}, and ϵ_{22}. Consider an elastic deformation of the interface at a constant temperature when one of the strain components, ϵ_{ij}, varies while other components are fixed. The interface stress obtained, which we denote $\hat{\tau}^{NV}$, represents the change in γA at a constant T and is given by

$$\tau_{ij}^{NV} = \frac{1}{A}\left[\frac{\partial(\gamma A)}{\partial e_{ij}}\right]_T = \frac{1}{A}[(\sigma_{ij}+\delta_{ij}p)V]_{NV} = \frac{1}{A}\frac{\begin{vmatrix}(\sigma_{ij}+\delta_{ij}p)V & N & V\\ (\sigma_{ij}^s+\delta_{ij}p)V^s & N^s & V^s\\ 0 & N^f & V^f\end{vmatrix}}{\begin{vmatrix}N^s & V^s\\ N^f & V^f\end{vmatrix}}. \quad (14)$$

This deformation is implemented along the isothermal path discussed in Part I,[2] on which p and μ^f vary in order to maintain equilibrium. For variations away from a hydrostatic state of the solid, the changes in p and μ^f were shown to be quadratic in nonhydrostatic components of the stress tensor in the solid.

In the second example, we choose $X=S$ and $Y=N$. This eliminates the differentials dT and $d\mu^f$ in the adsorption equation, which becomes

$$d(\gamma A) = [V]_{NS}dp + \sum_{ij=1,2}[(\sigma_{ij}+\delta_{ij}p)V]_{NS}d\epsilon_{ij}. \quad (15)$$

The independent variables are now p, ϵ_{11}, ϵ_{12}, and ϵ_{22} whereas T and μ^f vary to maintain equilibrium. By contrast to the previous case, the interface now has an excess volume $[V]_{NS}$.[26] The interface stress $\hat{\tau}^{NS}$ is defined through the work of elastic deformation at a constant pressure in the fluid

$$\tau_{ij}^{NS} = \frac{1}{A}\left[\frac{\partial(\gamma A)}{\partial e_{ij}}\right]_p = \frac{1}{A}[(\sigma_{ij}+\delta_{ij}p)V]_{NS} = \frac{1}{A}\frac{\begin{vmatrix}(\sigma_{ij}+\delta_{ij}p)V & N & S\\ (\sigma_{ij}^s+\delta_{ij}p)V^s & N^s & S^s\\ 0 & N^f & S^f\end{vmatrix}}{\begin{vmatrix}N^s & S^s\\ N^f & S^f\end{vmatrix}}. \quad (16)$$

The deformation path implied by Eq. (16) corresponds to the isobaric case discussed in Part I.[2] For variations away from a hydrostatic state of the solid, the changes in T and μ^f are quadratic in nonhydrostatic stresses in the solid.

The interface stresses $\hat{\tau}^{NV}$ and $\hat{\tau}^{NS}$ are generally different. They could be determined by measuring changes in γA during elastic deformations in two *different* thermodynamic processes: an isothermal and isobaric, respectively. Another possible interface stress is $\hat{\tau}^{SV}$, corresponding to elastic deformation at a constant chemical potential μ^f in the fluid (T and p vary to maintain equilibrium). We do not discuss this case in details but this interface stress can also be expressed as an appropriate excess of the nonhydrostatic stress tensor in a manner similar to $\hat{\tau}^{NV}$ and $\hat{\tau}^{NS}$.

2. Interface stress on an isofluid path

We will now introduce yet another definition of the interface stress. Let X or Y be one of the nonhydrostatic stresses $(\sigma_{ij}+\delta_{ij}p)V$. For example, suppose $Y=(\sigma_{22}+p)V$ while X is one of the extensive variables S, V, or N. This choice of Y eliminates $d\epsilon_{22}$ in Eq. (11) and reduces it to

$$d(\gamma A) = -[S]_{X(\sigma_{22}+p)V}dT + [V]_{X(\sigma_{22}+p)V}dp - [N]_{X(\sigma_{22}+p)V}d\mu^f + [(\sigma_{11}+p)V]_{X(\sigma_{22}+p)V}d\epsilon_{11} + [\sigma_{12}V]_{X(\sigma_{22}+p)V}d\epsilon_{12} + [\sigma_{21}V]_{X(\sigma_{22}+p)V}d\epsilon_{21}. \quad (17)$$

In this equation, one variable out of set (T,p,μ^f) is eliminated by specifying X, leaving four independent variables (recall that $\epsilon_{12}=\epsilon_{21}$). For example, $(T,p,\epsilon_{11},\epsilon_{12})$ or $(T,\mu^f,\epsilon_{11},\epsilon_{12})$ are possible sets of independent variables.

Note that if any two variables from the set (T,p,μ^f) are fixed, the third variable is also fixed because a single-component fluid has two degrees of freedom. A relation between these three variables is given by the Gibbs-Duhem Eq. (10). Thus, if any two variables from the set (T,p,μ^f) are held constant, γA can only vary due to the remaining strain terms, which represent the work of elastic deformation of the interface. This elastic work is done by an interface stress which we denote $\hat{\tau}^{(22)}$. The superscript (22) indicates the component of the strain tensor which is eliminated from the adsorption equation and becomes a dependent variable. The components of $\hat{\tau}^{(22)}$ are

$$\tau_{11}^{(22)} = \frac{1}{A}\left[\frac{\partial(\gamma A)}{\partial \epsilon_{11}}\right]_{T,p,\epsilon_{12}} = \frac{1}{A}[(\sigma_{11}+p)V]_{X(\sigma_{22}+p)V}, \quad (18)$$

$$\tau_{12}^{(22)} = \tau_{21}^{(22)} = \frac{1}{2A}\left[\frac{\partial(\gamma A)}{\partial \epsilon_{12}}\right]_{T,p,\epsilon_{11}} = \frac{1}{A}[(\sigma_{12}+p)V]_{X(\sigma_{22}+p)V} \quad (19)$$

whereas $\tau_{22}^{(22)}$ is identically zero due to the property of determinants [Eq. (6)].

Computing the determinants in Eqs. (18) and (19) explicitly,

$$\tau_{11}^{(22)} = \frac{1}{A}\frac{\begin{vmatrix}(\sigma_{11}+p)V & (\sigma_{22}+p)V & X\\ (\sigma_{11}^s+p)V^s & (\sigma_{22}^s+p)V^s & X^s\\ 0 & 0 & X^f\end{vmatrix}}{\begin{vmatrix}(\sigma_{22}^s+p)V^s & X^s\\ 0 & X^f\end{vmatrix}} = \frac{V}{A}\left\{(\sigma_{11}+p)-(\sigma_{11}^s+p)\frac{(\sigma_{22}+p)}{(\sigma_{22}^s+p)}\right\}, \quad (20)$$

$$\tau_{12}^{(22)} = \tau_{21}^{(22)} = \frac{1}{A}\frac{\begin{vmatrix} \sigma_{12}V & (\sigma_{22}+p)V & X \\ \sigma_{12}^{s}V^{s} & (\sigma_{22}^{s}+p)V^{s} & X^{s} \\ 0 & 0 & X^{f} \end{vmatrix}}{\begin{vmatrix} \sigma_{22}^{s}V^{s} & X^{s} \\ 0 & X^{f} \end{vmatrix}} = \frac{V}{A}\left\{\sigma_{12} - \sigma_{12}^{s}\frac{(\sigma_{22}+p)}{(\sigma_{22}^{s}+p)}\right\}. \quad (21)$$

Note that these expressions are independent of X.

Having introduced the interface stress $\hat{\tau}^{(kl)}$, we will now discuss the physical processes which can be implemented to measure it. The process to determine $\tau_{11}^{(22)}$ is a variation in ϵ_{11} at constant ϵ_{12}, T and p. In this process, μ^f is automatically fixed by the equation of state of the fluid. The remaining strain component ϵ_{22} is varied simultaneously with ϵ_{11} to maintain phase equilibrium. Likewise, $\tau_{12}^{(22)}$ and $\tau_{21}^{(22)}$ are determined in a process in which ϵ_{11}, T, p (and thus μ^f) are fixed while ϵ_{12} and ϵ_{22} vary simultaneously to maintain phase equilibrium. While the state of stress of the solid changes in these processes, the state of the fluid remains the same. Such processes were introduced in Part I of this work,[2] where they were called isofluid processes. Thus, $\hat{\tau}^{(kl)}$ can be referred to as isofluid interface stress.

There is a unique hydrostatic state of the solid, denoted H, in which it is equilibrated with a given fluid. It was shown[2] that no isofluid path can go through or originate from the hydrostatic point (T_H, p_H). Thus, $\hat{\tau}^{(kl)}$ is only defined for nonhydrostatic states of the solid.

Isofluid processes have the following geometric interpretation in the configuration space of variables. The isofluid constraints eliminate two degrees of freedom, leaving a single-component solid-fluid system with two remaining degrees of freedom. Isofluid states can be represented by a surface in the three-dimensional space of strain variables E_{11}, E_{12}, and E_{22}. The strain E_{ij} was introduced in Part I (Ref. 2) and is defined relative to the reference hydrostatic state (T_H, p_H). In the linear elasticity approximation, the isofluid surface is an ellipsoid centered at $E_{11}=E_{12}=E_{22}=0$ (Appendix C of Part I).[2]

To apply this analysis to atomistic simulations discussed later, let us consider a particular case in which E_{12} remains fixed at zero. Then the isofluid path is an ellipse in the coordinates E_{11} and E_{22}, which can be obtained as an intersection of the ellipsoid mentioned above with the plane $E_{12}=0$. Alternatively, this ellipse can be viewed as an intersection of two other surfaces. Specifically, at $E_{12}=0$ and a fixed pressure in the fluid, the solid-fluid coexistence surface is an elliptical paraboloid in the coordinates T versus E_{11} and E_{22} [Fig. 2(a)]. The equation of this paraboloid was derived in Appendix B of Part I.[2] The isofluid ellipse is obtained as an intersection of this paraboloid with a constant-temperature plane [Fig. 2(b)].

For any infinitesimal isofluid process on the ellipse, the solid phase is stretched by an amount dE_{11} and simultaneously compressed in the perpendicular direction by an amount dE_{22} in order to maintain equilibrium with the same fluid. Some of the equations involving the isofluid interface stress (see below) contain the slope of the isofluid curve. Since the reference state (T_H, p_H) is fixed during isofluid processes, the slope equals $dE_{22}/dE_{11}=d\epsilon_{22}/d\epsilon_{11}$, where the strain ϵ_{ij} is defined relative to the current state.

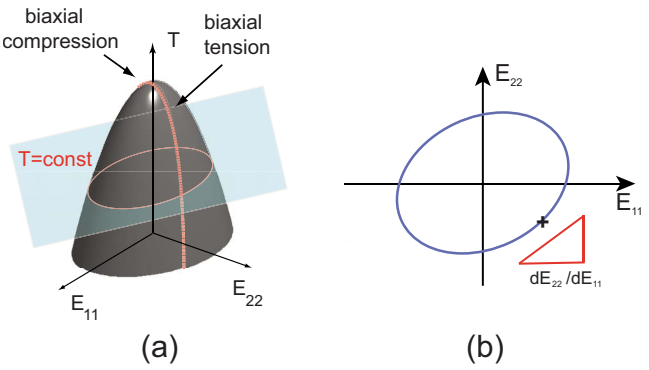

FIG. 2. (Color online) Equilibrium temperature T as a function of nonhydrostatic components of strain E_{ij} at a constant pressure p in the fluid and a constant E_{12}. (a) The line of biaxial tension/compression. (b) An iso-fluid path. The triangle shows the slope of the isofluid path at a particular point marked by a cross.

3. Relations between different interface stresses

In this section we analyze relations between different interface stresses. Such relations are readily obtained by equating right-hand sides of the adsorption equation for different choices of X and Y. Some of these relations will be later tested by atomistic simulations. We will limit the discussion to the particular case of $d\epsilon_{12}=0$.

Since there is no preference of choosing $d\epsilon_{11}$ over $d\epsilon_{22}$ as the independent variable to describe isofluid processes, we have two versions of the adsorption equation

$$d(\gamma A) = \tau_{11}^{(22)} d\epsilon_{11} = \tau_{22}^{(11)} d\epsilon_{22}. \quad (22)$$

It follows that the components $\tau_{11}^{(22)}$ and $\tau_{22}^{(11)}$ are proportional to each other,

$$\frac{\tau_{11}^{(22)}}{\tau_{22}^{(11)}} = \left(\frac{\partial \epsilon_{22}}{\partial \epsilon_{11}}\right)_{T,p,\epsilon_{12}}. \quad (23)$$

The slope of the isofluid curve [Fig. 2(b)] is assumed to be known from bulk thermodynamic properties. On the other hand, using Eq. (20) $\tau_{11}^{(22)}/\tau_{22}^{(11)}$ can be expressed as a ratio of nonhydrostatic components of stress in the solid,

$$\frac{\tau_{11}^{(22)}}{\tau_{22}^{(11)}} = \frac{\sigma_{11}^{s}+p}{\sigma_{22}^{s}+p}. \quad (24)$$

These relations permit useful cross-checks during interface stress calculations, which will be done in Sec. IV.

A relation between $\hat{\tau}^{NV}$ and $\hat{\tau}^{(22)}$ can be obtained by applying Eq. (13) to the particular case of an isofluid variation $(dT=0)$,

$$d(\gamma A) = \tau_{11}^{NV} d\epsilon_{11} + \tau_{22}^{NV} d\epsilon_{22}. \quad (25)$$

Because $d\epsilon_{11}$ and $d\epsilon_{22}$ must be proportional to each other to keep the system on the isofluid path, we can rewrite this equation as

$$d(\gamma A) = \left\{ \tau_{11}^{NV} + \tau_{22}^{NV} \left(\frac{\partial \epsilon_{22}}{\partial \epsilon_{11}} \right)_{T,p,\epsilon_{12}} \right\} d\epsilon_{11}. \tag{26}$$

Comparing this equation with Eq. (22), we obtain

$$\tau_{11}^{(22)} = \tau_{11}^{NV} + \tau_{22}^{NV} \left(\frac{\partial \epsilon_{22}}{\partial \epsilon_{11}} \right)_{T,p,\epsilon_{12}}. \tag{27}$$

This relation suggests another cross-check because $\hat{\tau}^{NV}$ and $\hat{\tau}^{(22)}$ can be computed independently.

The derivative $(\partial \epsilon_{22}/\partial \epsilon_{11})_{T,p,\epsilon_{12}}$ appearing in the above equations was computed in Part I (Ref. 2) in the linear elasticity approximation. It can be expressed through elastic constants of the solid phase and the strain E_{ij} relative to the hydrostatic state,

$$\left(\frac{\partial \epsilon_{22}}{\partial \epsilon_{11}} \right)_{T,p,\epsilon_{12}} = -\frac{A_{11}E_{11} + A_{12}E_{22}}{A_{22}E_{22} + A_{12}E_{11}}. \tag{28}$$

Here $A_{11} = C_{1111} - C_{1133}^2/C_{3333}$, $A_{22} = C_{2222} - C_{2233}^2/C_{3333}$, and $A_{12} = C_{1122} - C_{1133}C_{2233}/C_{3333}$, C_{ijkl} being the tensor of elastic constants in the hydrostatic state.

For each of the different interface stresses introduced in this work, there are points on the phase coexistence surface where the particular type of interface stress is undefined. For example, $\hat{\tau}^{(kl)}$ cannot be defined whenever $\sigma_{kl}^s + \delta_{kl}p = 0$, although τ^{NV}, τ^{NS}, and τ^{SV} generally remain well defined at such points. $\hat{\tau}^{NV}$ is undefined when a nonhydrostatic solid and a fluid have the same volume per atom (atomic density). Likewise, $\hat{\tau}^{NS}$ is undefined when entropy per atom is the same in both phases.

C. Relation to the Shuttleworth equation

The adsorption equation derived in Sec. II A 2 can be rewritten in a form similar to the Shuttleworth equation for open surfaces.[9] Taking the differential of γA in the left-hand side of Eq. (11) and using $dA = A \sum_{i,j=1,2} \delta_{ij} d\epsilon_{ij}$ we obtain

$$A d\gamma = -[S]_{XY} dT + [V]_{XY} dp - [N]_{XY} d\mu^f + \sum_{i,j=1,2} (\tau_{ij}^{XY} - \delta_{ij}\gamma) A d\epsilon_{ij}. \tag{29}$$

As before, two differentials in Eq. (29) are eliminated by specifying X and Y and the remaining differentials are independent. Taking a partial derivative of γ with respect to the elastic strain tensor while holding all the other independent variables fixed, we obtain[27]

$$\frac{\partial \gamma}{\partial \epsilon_{ij}} = \tau_{ij}^{XY} - \delta_{ij}\gamma. \tag{30}$$

In this equation, τ_{ij}^{XY} depends on the choice of X and Y. Accordingly, the derivative $\partial\gamma/\partial\epsilon_{ij}$ is taken along a path on the coexistence surface on which the intensive variables conjugate to the chosen X and Y are allowed to vary while all other variables are fixed. In effect, Eq. (30) represents a set of equations for different interface stresses τ_{ij}^{XY} and different partial derivatives $\partial\gamma/\partial\epsilon_{ij}$ taken along corresponding paths.

D. Thermodynamic integration methods

If γ is known at one point on the phase coexistence surface, the adsorption Eq. (11) can be integrated along a chosen path on this surface to compute γ as a function of intensive variables. However, if temperature varies along the path, the integration requires knowledge of the excess entropy $[S]_{XY}$. The latter is rarely accessible in experiments or simulations. To circumvent this problem, we combine Eqs. (4) and (11) to derive the interface version of the Gibbs-Helmholtz equation, which is more suitable for thermodynamic integration[8]

$$d\left(\frac{\gamma A}{T} \right) = -\frac{[\Psi]_{XY}}{T^2} dT + \frac{[V]_{XY}}{T} dp - \frac{[N]_{XY}}{T} d\mu^f + \frac{1}{T} \sum_{i,j=1,2} \tau_{ij}^{XY} d\epsilon_{ij}. \tag{31}$$

Here

$$\Psi \equiv U + pV - \mu^f N \tag{32}$$

is a thermodynamic potential that does not contain the entropy term. Just as the adsorption equation [Eq. (11)], Eq. (31) contains four independent variables. It can be integrated starting from a chosen reference point to recover γ along the path.

As an example, consider a path on the coexistence surface obtained by biaxial deformation of the solid at zero pressure p in the fluid. Due to the constraints $dp = 0$, $d\epsilon_{11} = d\epsilon_{22} \equiv d\epsilon$, and $d\epsilon_{12} = 0$, we have only one independent variable. Choosing T as the independent variable, Eq. (31) is readily integrated to give

$$\gamma A = \frac{(\gamma A)_0 T}{T_0} - T \int_{T_0}^{T} \left[\frac{(U)_{NV}}{T'^2} - \frac{(\tau_{11}^{NV} + \tau_{22}^{NV})}{T'} \left(\frac{\partial \epsilon}{\partial T'} \right)_{coex.} \right] dT'. \tag{33}$$

Here $(\gamma A)_0$ and T_0 are the reference values of the total interface free energy and temperature. The derivative $(\partial\epsilon/\partial T)_{coex}$ is taken along the coexistence path. An advantage of Eq. (33) is that all quantities appearing in the integrand are readily accessible in atomistic calculations.

Consider another integration path on which pressure is fixed at zero. Choosing $X = N$, Eq. (31) reduces to

$$d\left(\frac{\gamma A}{T} \right) = -\frac{[U]_{NY}}{T^2} dT + \frac{1}{T} \sum_{i,j=1,2} \tau_{ij}^{NY} d\epsilon_{ij}. \tag{34}$$

Taking U for Y and integrating, we obtain

$$\gamma A = \frac{(\gamma A)_0 T}{T_0} + T \int_{T_0}^{T} \left[\frac{(\sigma_{11} + p)_{NU} + (\sigma_{22} + p)_{NU}}{T'} \left(\frac{\partial \epsilon}{\partial T'} \right)_{coex.} \right] dT'. \tag{35}$$

This integration path requires calculation of only two excess quantities, $[\sigma_{11} + p]_{NU}$ and $[\sigma_{22} + p]_{NU}$, instead of three in Eq. (33). Calculations of excesses $[Z]_{NU}$ instead of $[Z]_{NV}$ have

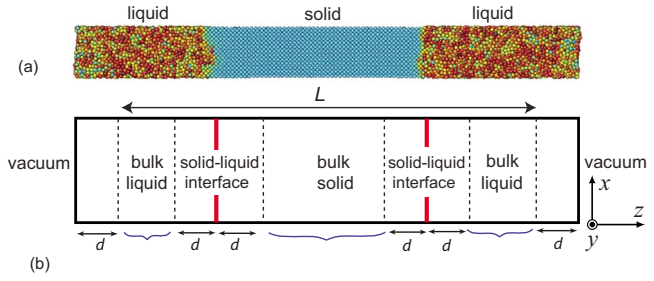

FIG. 3. (Color online) (a) Typical snapshot of the simulation block with the solid and liquid phases. (b) Schematic illustration of regions selected for calculations of excess quantities.

some computational advantages in atomistic simulations. Both Eqs. (33) and (35) will be used below to compute the interface free energy along biaxial tension and compression paths at zero pressure in the liquid.

III. METHODOLOGY OF ATOMISTIC SIMULATIONS

A. Simulation block and molecular dynamics methodology

As in Part I,[2] we used copper as a model material with atomic interactions described with an embedded-atom potential.[28] The potential predicts the melting temperature $T_H=1327$ K at zero pressure, which is close to the experimental melting point 1356 K.[29]

The simulation block with dimensions $x\times y\times z=32\times 30\times 325$ Å^3 contained the total of 23 040 atoms. A 105 Å thick layer of the solid phase was located in the middle of the block between two 110 Å thick liquid layers [Fig. 3(a)]. The solid and liquid phases were separated by (110) oriented solid-liquid interfaces perpendicular to the z direction. The $[\bar{1}10]$ and [001] crystallographic directions in the solid were parallel to the x and y axes, respectively. The boundary conditions in the x and y directions were periodic, with the free surface condition in the z direction. The termination of the liquid layers at open surfaces ensured constant zero pressure in the liquid phase ($p=0$).

To create nonhydrostatic stresses in the solid phase, the block was subject to biaxial deformation parallel to the interface. Eleven simulation blocks were prepared with different biaxial tensions and compressions. The lateral stresses created in the solid layer ranged from −2.1 GPa (compression) to 3.4 GPa (tension). The normal stress σ_{33} remained zero due to mechanical equilibrium with the liquid.

After application of the deformation, each simulation block was equilibrated by a 2 ns *NVE* molecular dynamics (MD) run. We refer the reader to Part I (Ref. 2) for details of the equilibration procedure. The obtained equilibrium temperature and lateral stresses in the solid were functions of the applied deformation. In the linear elasticity approximation, T is a paraboloid as a function of the lateral strains E_{11} and E_{22} as shown schematically in Fig. 2(a).[2] The red dashed line indicates the biaxial deformation path implemented in this work. The equilibration step was followed by a 40 ns production run (also in the *NVE* ensemble) with snapshots generated every 0.01 ns. The snapshots contained coordinates, energies and stresses for all atoms and were used for post-processing.

B. Calculation of profiles and excess quantities

Profiles of energy, atomic density and stress components as functions of distance in the z direction provide useful information about internal structure of the interface region. To compute such profiles, each snapshot was divided into bins of equal width and the property of interest was averaged within each bin. To obtain smooth profiles, each atom was smeared into a Gaussian along the z axis. Properties related to each atom, such as density, energy, and stress, were distributed over its vicinity with the Gaussian distribution.

During an MD run, the position of the interface constantly changes due to thermal fluctuations. The interface implements a random walk along the z axis by spontaneous melting and crystallization processes within thin layers adjacent to the interface.[30] This interface motion can result in a broadening of the profiles. To avoid the broadening, the interface motion was monitored by computing profiles of the structure factor $|S(\mathbf{k})|$ ($\mathbf{k}$ being a suitable vector of reciprocal lattice), which gave us an approximate interface position in every snapshot.[7,8] The profiles of other properties computed for individual snapshots were centered relative to the instantaneous position of the interface as identified by $|S(\mathbf{k})|$ and then averaged. After computing the averaged profiles of all properties, they were shifted so that the Gibbsian dividing surface determined from the density profile was at $z=0$. This shift is dictated by convenience of presentation of profiles and does not constitute any approximation of our analysis.

All excess quantities, such as the interface stress, excess energy, etc., were calculated from Eq. (5). Each entry of the determinants was computed for individual snapshots and then averaged. Such entries represented extensive quantities that were computed for selected regions of the simulation block. Properties of individual atoms continued to be represented by Gaussians. The profiles of $|S(\mathbf{k})|$ were used as a guide during the region selection as they indicated approximate positions of the solid-liquid interfaces. The liquid surfaces were identified with the maximum and minimum values of the z coordinate of atoms. An inner region of the solid layer separated by a distance d from both solid-liquid interfaces was taken as the bulk solid region [Fig. 3(b)]. Two liquid regions separated by d from the solid-liquid interfaces and from the liquid surfaces represented by the bulk liquid phase. Finally, the region containing two solid-liquid interfaces and separated by a distance d from the liquid surfaces was selected as the interface layer. In Fig. 3(b) this layer is labeled by L. Since boundaries of the regions were placed relative to the instantaneous positions of the interfaces and surfaces, they slightly varied from one snapshot to the next. Due to properties of determinants in Eq. (5), the locations of the boundaries do not affect the excesses as long as these boundaries are within homogeneous phases.[6] A choice of $d=20$ Å was found to satisfy this condition. Note that the profiles of properties discussed above were not used for interface excess calculations. They were constructed for illustration purposes only.

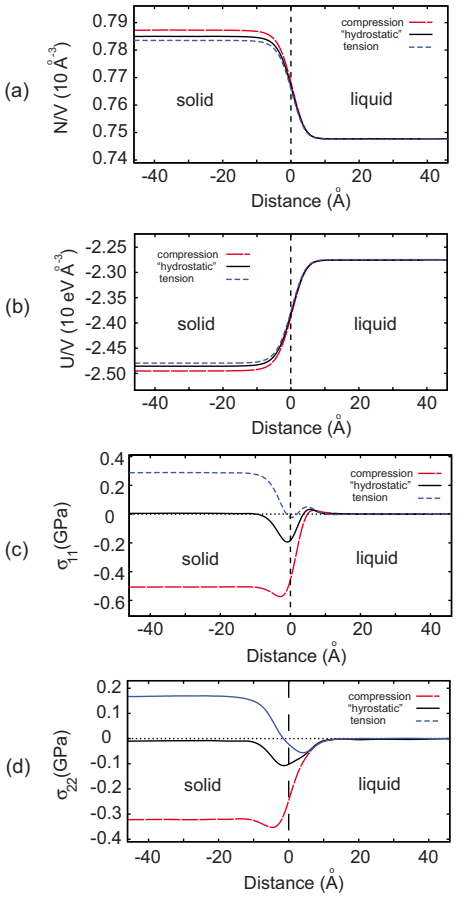

FIG. 4. (Color online) Profiles of (a) atomic density, (b) energy density, and stress components (c) σ_{11} and (d) σ_{22} when the solid is under compression (T=1325.2 K), tension (T=1325.5 K) and nearly hydrostatic (T=1326.4 K). The vertical dashed line indicates the position of the Gibbsian dividing surface.

IV. RESULTS

Figures 4(a) and 4(b) display typical profiles of atomic density and energy density across the simulation block when the solid phase is under tension, under compression and nearly hydrostatic. The profiles shown in Fig. 4(b) reveal that the internal energy in the solid decreases with biaxial compression. This is not surprising since quadratic behavior of energy with applied biaxial strain is not expected in this case. It is the free energy that is quadratic in strain and stress whereas the internal energy is linear. Figures 4(c) and 4(d) show the corresponding profiles of the stress components σ_{11} and σ_{22}. These two components exhibit different behaviors in the interface region. The σ_{11} component has a peak of compression on the solid side of the Gibbsian dividing surface accompanied by a peak of slight tension on the liquid side. By contrast, σ_{22} shows a single compressive peak. Note also that the magnitudes of the stress components inside the solid are significantly different, which is explained by the anisotropy of elastic constants. The overall thickness of the nonhomogeneous interfacial region is about 20 Å.

The excess energy per unit area, $[U]_{NV}/A$, which is needed for thermodynamic integration by Eq. (33), is plotted in Fig. 5 as a function of biaxial compression and tension.

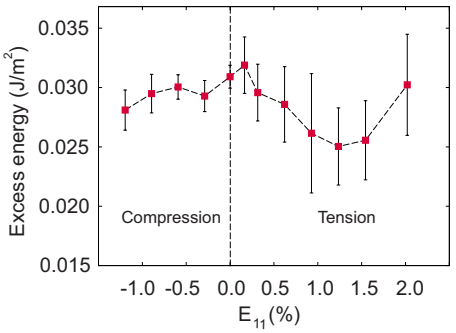

FIG. 5. (Color online) Excess energy per unit area, $[U]_{NV}/A$, as a function of biaxial strain. The vertical dashed line indicates the stress-free state of the solid phase.

Within the relatively narrow temperature range implemented in this work, $[U]_{NV}/A$ does not change significantly. It slightly decreases as the solid deviates from the hydrostatic state but increases again under a larger tension. The magnitude of $[U]_{NV}/A$ is nearly an order of magnitude smaller than the interface free energy (see below).

The diagonal components of the interface stress $\hat{\tau}^{NV}$ are shown in Fig. 6 as functions of biaxial strain. When the solid is hydrostatic, the interface stress is only slightly anisotropic with the components $\tau_{11}^{NV}=-0.105\pm0.004$ J/m^2 and $\tau_{22}^{NV}=-0.110\pm0.002$ J/m^2.[31] The negative sign indicates that the interface is in a state of compression. As the solid deviates from the hydrostatic state, the anisotropy of $\hat{\tau}^{NV}$ increases significantly. A reversal of the bulk stress from compression to tension changes the sense of the anisotropy. It should be mentioned, however, that the average of τ_{11}^{NV} and τ_{22}^{NV} is much less affected by the applied stresses than the individual components.

Figure 7 shows a plot of the isofluid interface stresses $\tau_{11}^{(22)}$ and $\tau_{22}^{(11)}$ as functions of lateral strain. Both stresses were computed from Eq. (20) with switches between indices (11) and (22). Note that these two stresses have different signs which change within the simulated range of lateral strains. As discussed in Sec. II B 3, the ratio of these interface stresses equals $(\partial\epsilon_{22}/\partial\epsilon_{11})_{T,p,\epsilon_{12}}$, which has the meaning of the slope of the isofluid path in the coordinates E_{11} and E_{22}. In the linear elasticity approximation, the derivative $(\partial\epsilon_{22}/\partial\epsilon_{11})_{T,p,\epsilon_{12}}$ must be constant along a biaxial deforma-

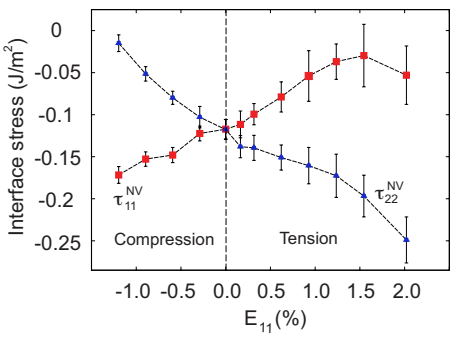

FIG. 6. (Color online) Components of the interface stress $\hat{\tau}^{NV}$ as functions of biaxial strain. The vertical dashed line indicates the stress-free state of the solid phase.

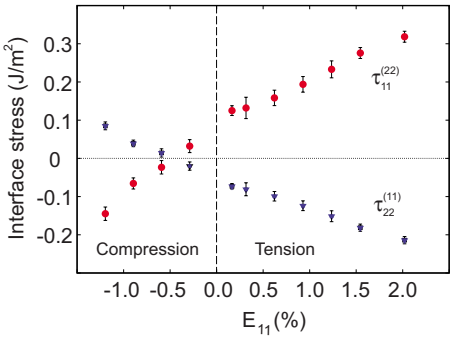

FIG. 7. (Color online) Isofluid interface stresses as functions of biaxial strain. The vertical dashed line indicates the stress-free state of the solid phase.

tion path. This constant value was calculated from Eq. (28) using the elastic constants of the solid determined in Part I (Ref. 2) at the temperature T_H. The value obtained, $(\partial\epsilon/\partial\epsilon_{11})_{T,p,\epsilon_{12}}=-1.62$, is shown by the dashed line in Fig. 8. The individual points on this plot are the ratios $\tau_{11}^{(22)}/\tau_{22}^{(11)}$ computed for different states of tension and compression. Although the points display noticeable deviations from the predicted line, the relation (23) is approximately followed. There can be several reasons for the discrepancy, including deviations from linear elasticity, the system size effect and other factors. It should be noted that reducing the magnitude of the applied strain does not improve the accuracy of the calculations because the isofluid ellipse becomes too small (Fig. 2). In the limit of a hydrostatic solid, the ellipsoid shrinks to a point and the ratio $(\partial\epsilon_{22}/\partial\epsilon_{11})_{T,p,\epsilon_{12}}$ becomes undefined.

Finally, Fig. 9 reports the temperature dependence of the interface free energy γ obtained by thermodynamic integration of Eqs. (33) and (35). As the reference state we used the hydrostatic solid-liquid coexistence at $p=0$. The interface free energy for this state, 0.199 J/m^2, was computed in our previous work.[7] To find the derivative $(\partial\epsilon/\partial T)_{coex}$ appearing in Eqs. (33) and (35), the previously obtained[2] biaxial strain ϵ as a function of T was fitted with a cubic spline and differentiated numerically. Figure 9 shows that the interface free energy decreases under biaxial tension but increases under biaxial compression. In the latter case, it reaches a maximum at 1307 K and apparently reverses. In the range of strains studied in this work, the maximum decrease in γ under tension is 9.1% and the maximum increase under compression is 2.3%. Thus, the effect of nonhydrostaticity on γ is much weaker than the effect on the interface stresses. As expected, the values of γ computed by the different integration methods are identical within the accuracy of the calculations.

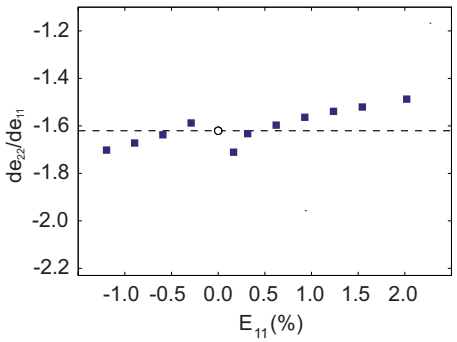

FIG. 8. (Color online) The slope of the isofluid path as a function of biaxial strain. The value −1.62 computed from Eq. (28) is shown by the horizontal dashed line. The open circle is a reminder that the slope is undefined for the hydrostatic state.

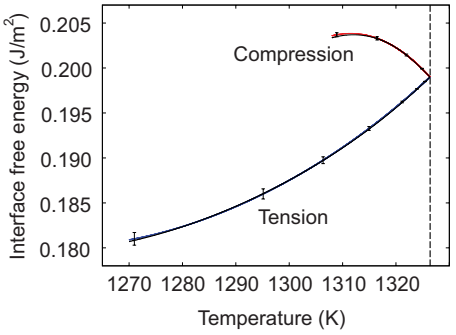

FIG. 9. (Color online) Interface free energy γ as a function of equilibrium temperature T for biaxial compression and tension. The red and blue lines were computed from Eq. (33) while the black line was computed using Eq. (35). The results of the two calculations coincide within the error of integration. The vertical dashed line indicates the stress-free state of the solid phase.

V. SUMMARY AND CONCLUSIONS

We have studied thermodynamics solid-fluid interfaces in a single-component system in the presence of nonhydrostatic stresses in the solid phase. While some aspects of this analysis can be found in our previous paper dedicated to binary systems,[8] the present study was focused on the multiplicity of definitions of the interface stress $\hat{\tau}$ and its dependence on applied bulk stresses. The interface stress is generally defined as reversible work of elastic deformation of the interface. More specifically, it is defined through the term in the adsorption equation which is responsible for elastic deformations of the interface. We have shown how this term can be expressed as an interface excess quantity similar to excesses of energy, entropy, volume, and other properties. The extensive property whose excess per unit area gives the interface stress is the tensor $(\sigma_{ij}+\delta_{ij}p)V$ representing nonhydrostatic stresses in the system (p being pressure in the fluid).

The physical origin of the nonuniqueness of $\hat{\tau}$ is in the fact that the elastic deformations implied by its definition can be implemented under different conditions. Thus, one can talk about an isothermal interface stress $\hat{\tau}^{NV}$, isobaric $\hat{\tau}^{SV}$, or an open-system interface stress $\hat{\tau}^{SV}$ (Sec. II B 1). As another example, $\hat{\tau}$ can be defined through an isofluid process, in which two or more components of strain vary simultaneously while the state of the fluid remains the same. Furthermore, because of the multiplicity of possible isofluid deformation paths, there is a multiplicity of isofluid interface stresses $\hat{\tau}^{(kl)}$. It is important to note that the interface stresses not only differ conceptually but can also have different magnitudes or even signs. Thus, care should be exercised when comparing

interface stresses obtained by different measurements or simulations. It is only when the solid is hydrostatic that $\hat{\tau}$ has a unique value.

Mathematically, the nonuniqueness of $\hat{\tau}$ arises from the freedom of choice of the independent intensive variables in the adsorption equation. This choice is controlled through the selection of two extensive properties X and Y in the definition of excess quantities by Eq. (5). Depending of this choice, different variables are held constant during the deformation, leading to different definitions of $\hat{\tau}$. By analyzing various choices of variables in the adsorption equation, relationships between different interface stresses can be established as discussed in Sec. II B 3. Such relations can be useful for cross-checking results of different experiments or simulations. It should also be pointed out that the formalism presented in this work automatically guarantees that the deformation paths chosen for the definition of $\hat{\tau}$ lie on the phase coexistence surface and are consistent with the Gibbs phase rule. This helps avoid meaningless definitions, such as the derivative $\tau_{ij}=(\partial\gamma A/\partial\epsilon_{ij})_{p,T}$ which cannot be obtained from Eq. (11) and constitutes an impossible variation (a change of a single component of strain at fixed other components, p and T destroys the phase coexistence).

We have applied molecular dynamics simulations to compute several different interface stresses for a (110) solid-liquid interface in copper. The solid phase was subject to biaxial tension and compression producing nonhydrostatic stresses reaching the gigapascal level. These nonhydrostatic stresses were found to strongly affect the magnitude, anisotropy, and even sign of various interface stresses. As expected from the above analysis, differently defined interface stresses were found to be very different in magnitude, anisotropy, and sign. By contrast, the interface free energy is much less sensitive to nonhydrostatic stresses. This observation can be of interest for understanding various interface phenomena, some of which are controlled by the interface free energy while others by interface stress. We hope that this work will motivate further analysis of such phenomena and their dependence on applied stresses.

ACKNOWLEDGMENTS

This work was supported by the U.S. Department of Energy, Office of Basic Energy Sciences. We acknowledge useful discussions facilitated through coordination meetings sponsored by the DOE-BES Computational Materials Science Network (CMSN) program.

*tfrolov@gmu.edu
†ymishin@gmu.edu

[1] Y. Mishin, M. Asta, and J. Li, Acta Mater. **58**, 1117 (2010).
[2] T. Frolov and Y. Mishin, preceding paper, Phys. Rev. B **82**, 174113 (2010).
[3] J. W. Gibbs, *The Collected Works of J. W. Gibbs* (Yale University Press, New Haven, 1948), Vol. 1.
[4] R. C. Cammarata, Philos. Mag. **88**, 927 (2008).
[5] R. C. Cammarata, in *Solid State Physics*, edited by H. Ehrenreich and F. Spaepen (Elsevier Academic Press, Burlington, 2009), Vol. 61, pp. 1–75.
[6] J. W. Cahn, in *Interface Segregation*, edited by W. C. Johnson and J. M. Blackely (American Society of Metals, Metals Park, OH, 1979), Chap. 1, p. 3.
[7] T. Frolov and Y. Mishin, Phys. Rev. B **79**, 045430 (2009).
[8] T. Frolov and Y. Mishin, J. Chem. Phys. **131**, 054702 (2009).
[9] R. Shuttleworth, Proc. Phys. Soc., London, Sect. A **63**, 444 (1950).
[10] J. Q. Broughton and G. H. Gilmer, J. Chem. Phys. **84**, 5759 (1986).
[11] R. L. Davidchack and B. B. Laird, Phys. Rev. Lett. **85**, 4751 (2000).
[12] J. J. Hoyt, M. Asta, and A. Karma, Phys. Rev. Lett. **86**, 5530 (2001).
[13] J. Morris and X. Song, J. Chem. Phys. **116**, 9352 (2002).
[14] C. A. Becker, D. L. Olmsted, M. Asta, J. J. Hoyt, and S. M. Foiles, Phys. Rev. B **79**, 054109 (2009).
[15] B. B. Laird, R. L. Davidchack, Y. Yang, and M. Asta, J. Chem. Phys. **131**, 114110 (2009).
[16] B. B. Laird and R. L. Davidchack, J. Chem. Phys. **132**, 204101 (2010).
[17] S. Angioletti-Uberti, M. Asta, M. W. Finnis, and P. D. Lee, Phys. Rev. B **78**, 134203 (2008).
[18] S. Angioletti-Uberti, M. Ceriotti, P. D. Lee, and M. W. Finnis, Phys. Rev. B **81**, 125416 (2010).
[19] X. M. Bai and M. Li, J. Chem. Phys. **123**, 151102 (2005).
[20] X. M. Bai and M. Li, J. Chem. Phys. **124**, 124707 (2006).
[21] V. G. Baidakov, A. O. Tipeev, K. S. Bobrov, and G. V. Ionov, J. Chem. Phys. **132**, 234505 (2010).
[22] This definition is valid for single-component systems. Multicomponent systems require a separate treatment (Ref. 8).
[23] Out of the four differentials $d\epsilon_{ij}$, only three are independent due to the symmetry of tensor ϵ_{ij}.
[24] A generally stressed single-component solid has seven degrees of freedom, e.g., T and σ^s_{ij}. Mechanical equilibrium with the fluid requires that σ^s_{13} and σ^s_{23} be identically zero, imposing two constraints.
[25] Although ϵ_{ij} is a symmetric tensor, the partial derivative $\partial(\gamma A)/\partial\epsilon_{ij}$ is taken by *formally* treating the four components of ϵ_{ij} as independent variables.
[26] If related per unit area, excess volume of an interface is the relative rigid translation of the phases normal to the interface during its formation.
[27] Although ϵ_{ij} is a symmetric tensor, the partial derivative $\partial\gamma/\partial\epsilon_{ij}$ is taken by *formally* treating the four components of ϵ_{ij} as independent variables.
[28] Y. Mishin, M. J. Mehl, D. A. Papaconstantopoulos, A. F. Voter, and J. D. Kress, Phys. Rev. B **63**, 224106 (2001).
[29] *Binary Alloy Phase Diagrams*, edited by T. B. Massalski (ASM, Materials Park, OH, 1986).
[30] In the *NVE* ensemble, the walks of the two interfaces are not completely random. They are constrained to keep the average amount of each phase constant.
[31] T. Frolov and Y. Mishin, Modell. Simul. Mater. Sci. Eng. **18**, 074003 (2010).